Int. J. Electrochem. Sci., 14 **(2019)** 2063 – 2084, doi: 10.20964/2019.02.08

International Journal of
ELECTROCHEMICAL
SCIENCE
www.electrochemsci.org

Corrosion Inhibition of Sabic Iron in Different Media Using Synthesized Sodium N-dodecyl Arginine Surfactant

A. Fawzy[1,2,*], *M. Abdallah*[1,3], *M. Alfakeer*[4], *H. M. Ali*[5]

[1] Chemistry Department, Faculty of Applied Science, Umm Al-Qura University, Makkah, Saudi Arabia
[2] Chemistry Department, Faculty of Science, Assiut University, Assiut, Egypt
[3] Chemistry Department, Faculty of Science, Benha University, Benha, Egypt
[4] Chemistry Department, Faculty of Science, Princess Nourah bint Abdulrahman University, Riyadh, Saudi Arabia
[5] Chemistry Department, Faculty of Science, Jouf University, Jouf, Saudi Arabia
[*]E-mail: afsaad13@yahoo.com

Received: 14 October 2018 / *Accepted:* 3 December 2018 / *Published:* 5 January 2019

Sodium N-dodecyl arginine surfactant (sodium 2-(dodecylamino)-5-guanidinopentanoate) was synthesized and examined as an inhibitor for the corrosion of Sabic iron in acidic (HCl), neutral (NaCl) and alkaline (NaOH) media using different techniques, namely, weight-loss (WL), potentiodynamic polarization (PP) and electrochemical impedance spectroscopy (EIS). Increasing the concentrations of the acidic, neutral and alkaline media increased the corrosion rates of Sabic iron and increased the corrosion rate in the order: HCl >> NaCl > NaOH. It was found that the inhibition efficiency of the inhibitor increased with the concentration of the inhibitor while decrease with raising temperature. The results indicate that the inhibition efficiency of the inhibitor increased in the studied media in the sequence: HCl > NaCl > NaOH. The high inhibition efficiency of arginine surfactant inhibitor was interpreted on the basis of strong adsorption of the inhibitor molecules on the surface of Sabic iron and forming a protective film. The adsorption was found to obey Langmuir adsorption isotherm. The evaluated thermodynamic and kinetic parameters support the mechanism of physical adsorption of the inhibitor. The results obtained from all used techniques are in a good agreement with each others.

Keywords: Sabic iron, corrosion, sodium N-dodecyl arginine surfactant, inhibitor, adsorption.

1. INTRODUCTION

Different types of steel alloys such as carbon steel, mild steel, Sabic iron, … etc, are a major building materials and are widely used in a broad areas of industrial applications, and almost in everyday

life because of their good mechanical properties. However, these steel alloys and other metals and alloys suffer from corrosion phenomena in some environments [1]. Corrosion of metals and alloys is a serious problem and it is receiving more attention by corrosion scientists all over the world because of its dual impacts on both economy and safety. The use of corrosion inhibitors is considered as the most effective and economical way to protect the surfaces of metals against corrosion in aggressive media [2-9]. Inhibitors are adsorbed on the metal surface to form a protective film acting as a barrier between the metal surface and the corrosive medium [1].

Surfactants have been reported as corrosion inhibitors for various metals and alloys, and several mechanisms for inhibition were proposed [10-12]. Biosurfactants are organic molecules having various medical applications [13-15]. Amino acid-based surfactants are regarded as an interesting category of biosurfactants with excellent adsorption and aggregation properties. Various amino acid-based surfactants have been synthesized earlier by Pérez et. al [16-18] and in our laboratory [19,20]. L-arginine, an essential amino acid, which is a precursor for nitric oxide, urea, creatine and many other pharmacologically important molecules, thus it is widely used in pharmaceuticals and biochemical research [21].

In this investigation we aim to design, synthesize a new surfactant based on the amino acid arginine, namely, sodium N-dodecyl arginine surfactant (ArS) (Sodium 2-(dodecylamino)-5-guanidinopentanoate) shown below, and examine it as a corrosion inhibitor for Sabic iron in acidic, neutral and alkaline media using various techniques.

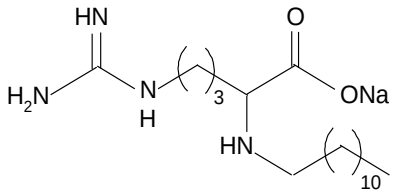

Sodium *N*-dodecyl arginine surfactant

2. EXPERIMENTAL

2.1. Materials

In this investigation all solutions were prepared afresh from Merck or Aldrich chemicals and double distilled water. Solutions of the corrosive media (HCl, NaCl and NaOH) were prepared with double distilled water. The new inhibitor (sodium N-dodecyl arginine surfactant) was synthesized as reported earlier [17-20]. The chemical structure of the synthesized surfactant (ArS) was characterized by using FT-IR spectroscopic tool and is shown in Fig. 1. The FT-IR spectrum of the compound (**I**), L-arginine, showed the absorption bands around 3275 cm^{-1} (for NH groups) and at about 1730 cm^{-1} for the ester carbonyl group while the compound (**II**) is the synthesized surfactant. The inhibitor was used in the concentration range 100-900 ppm (mgl^{-1}). Each experiment was repeated 3 times to check the

reproducibility. Corrosion tests were performed on a cylindrical Sabic iron specimens which has chemical composition listed in Table 1.

Table 1. Compositions (wt. %) of the investigated Sabic iron specimen.

Element	C	Mn	S	P	Si	Al	Cr	Cu	Mo	Ni	Fe
Weight (%)	0.046	0.175	0.010	0.008	0.009	0.039	0.0126	0.034	0.0026	0.0293	balance

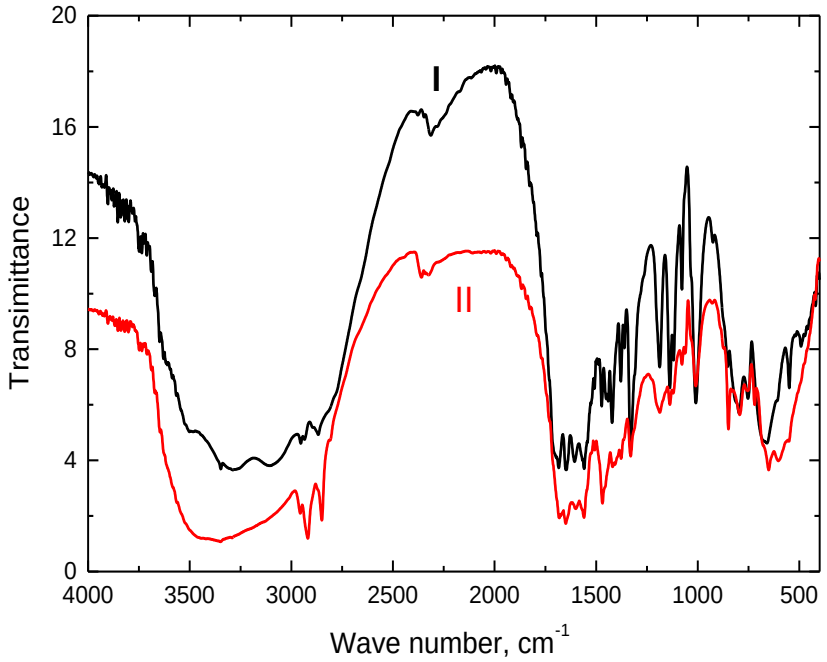

Figure 1. FT-IR spectra of L-arginine (**I**) and sodium N-dodecyl arginine surfactant (**II**).

2.2. Weight-Loss (WL) Measurements

WL measurements were carried out in a thermostated system. Sabic iron specimens used for WL measurements were cylindrical rods of areas closed to 10 cm^2. Such rods were prepared for these measurements as follows: polishing the rods with emery papers in successive grades from 200 to 1200, washing them with distilled water and acetone. After weighing the Sabic iron specimens, they were immersed in the corrosive media (in the absence and presence of different concentrations of the synthesized inhibitor) and at different temperatures. After 6 h, the Sabic iron specimens were taken out, washed, dried and weighed accurately. Thus, the average WL of three Sabic iron specimens, in each experiment, were obtained. The corrosion rate (CR) was calculated in mpy from the following equation [22]:

$$CR = \frac{KW}{Atd} \quad (1)$$

where K is a constant equals to 3.45 x 10^6, W is the specimen weight loss in grams, A is the specimen area in cm^2, t is time in hours and d is the specimen density in g/cm^3. The inhibition efficiency (% IE) of the inhibitor were calculated by the following equation [23]:

$$\% \text{ IE} = \theta \text{ x } 100 = \left[1 - \frac{CR_{inh}}{CR}\right] \text{ x } 100 \qquad (2)$$

where CR and CR_{inh} are the corrosion rate of specimens without and with inhibitor, respectively.

2.3. Electrochemical Measurements

Both PP and EIS measurements were performed by using PGSTAT30 potentiostat/galvanostat in a thermostated system in a double-jacket three-electrode cell. The working electrode was a rod of Sabic iron pressed into a Teflon holder in which the exposed electrode area to the corrosive media was 0.5 cm^2. Before each experiment the working electrode was treated as in WL, then it was inserted into the corrosive medium (blank) and/or the required inhibitor concentration at open circuit potential (OCP) for about 60 min or until a steady state was attained. In PP, the electrode potential was automatically changed in a potential range of -200 mV to +200 mV vs. OCP at a scan rate of 2.0 mV/s. The values of % IE of the inhibitor were calculated from the following equation:

$$\% \text{ IE} = \theta \text{ x } 100 = \left[1 - \frac{i_{corr\,(inh)}}{i_{corr}}\right] \text{ x } 100 \qquad (3)$$

where, i_{corr} and $i_{corr(inh)}$ are the corrosion current densities.

EIS measurements were performed in a frequency range of 100 kHz to 0.1 Hz with an amplitude of 4.0 mV peak-to-peak using AC signals at OCP. % IE values were evaluated by the equation [24]:

$$\% \text{ IE} = \left[1 - \frac{R_{ct}}{R_{ct\,(inh)}}\right] \text{ x } 100 \qquad (4)$$

where R_{ct} and $R_{ct(inh)}$ are the values of charge transfer resistance in ohms cm^2.

2.4. Surface Investigations

Investigation of the morphology of Sabic iron surface before and after addition of the inhibitor was performed by scanning electron microscopy (SEM) to show whether the inhibitor adsorbed on the surface of Sabic iron or just peeled off it.

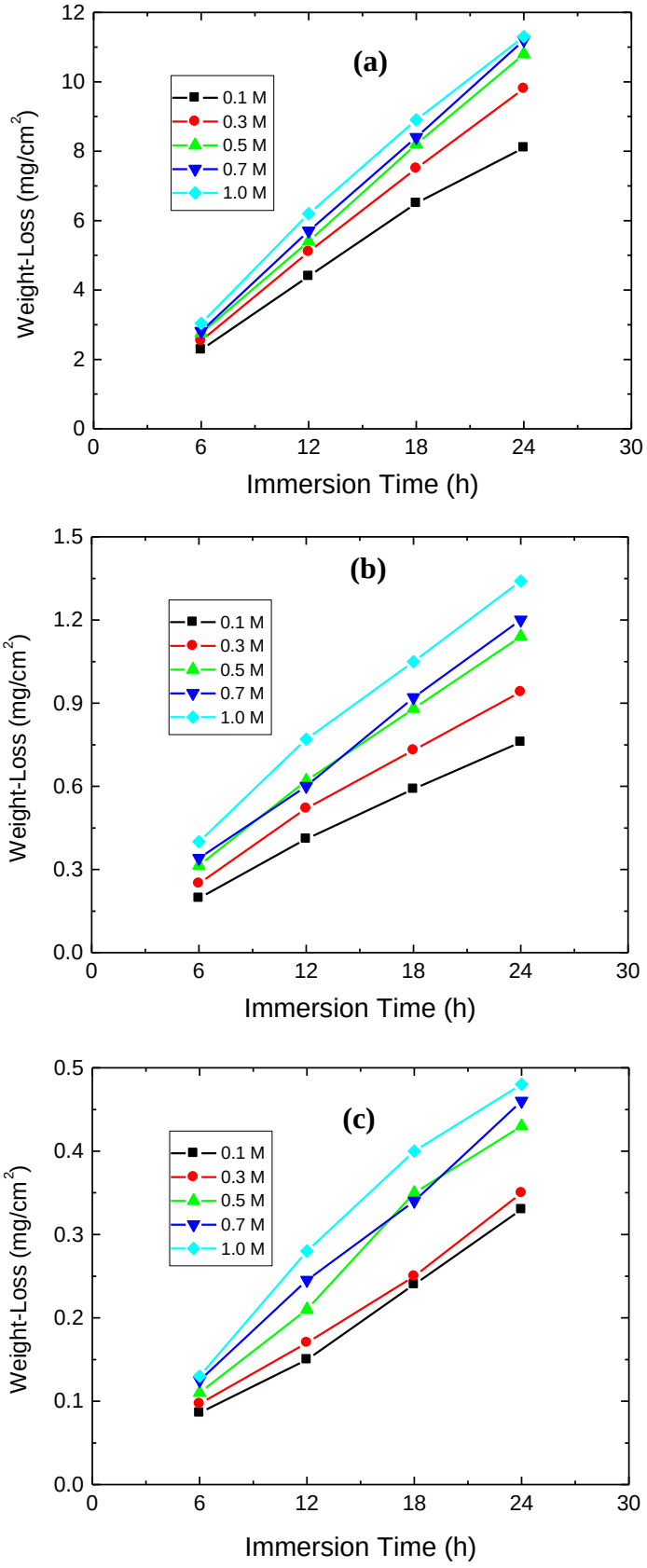

Figure 2. Weight-loss against immersion time for Sabic iron in the corrosive media at 25 ^{o}C. (a) HCl, (b) NaCl and (C) NaOH.

3. RESULTS AND DISCUSSION

3.1. Weight-Loss (WL) Measurements

3.1.1. Effect of Corrosive Media

Results of WL measurements for Sabic iron in different concentrations of the corrosive media (HCl, NaCl and NaOH) in the range of (0.1 – 1.0 M) at 25 ^{o}C are represented in Figure 2 and the values of the corrosion rates are inserted in Table 2. Corrosion rates of Sabic iron were found to increase with the increase in the concentration of the studied corrosive media. Also, corrosion rates of Sabic iron were found to increase in the corrosive media in the order: HCl >> NaCl > NaOH.

Table 2. Corrosion rates in mpy for Sabic iron in the corrosive media (HCl, NaCl and NaOH) at 25 ^{o}C.

Concn. (mol dm^{-3})	**HCl**	**NaCl**	**NaOH**
0.1	166.9	14.5	6.3
0.3	186.2	18.3	7.1
0.5	202.0	23.1	8.2
0.7	205.7	25.2	9.2
1.0	223.1	29.7	9.5

3.1.2. Effect of Inhibitor Concentration

WL measurements of Sabic iron in 0.5 M of the corrosive media (HCl, NaCl and NaOH) were carried out in the absence and presence of surfactant inhibitor (sodium N-dodecyl arginine (ArS)) in the concentration range: 100 to 900 ppm at four temperatures (15, 25, 35 and 45 ^{o}C); WL - time curves obtained at 25 ^{o}C are only shown here, Figure 3. The values of the CR, % IE and θ of the inhibitor are also listed in Table 3. The results indicated that CR values decreased with the inhibitor concentration.

This behavior is due to increased adsorption coverage of the inhibitor on the surface of Sabic iron with the inhibitor concentrations which decreases the dissolution rates of Sabic iron by blocking the corrosion sites present on the iron surface. Thus, the synthesized arginine surfactant can be considered as an efficient inhibitor for the corrosion of Sabic iron in the investigated aggressive media. At the same concentration of the inhibitor, the inhibition efficiencies follows the order: HCl > NaCl > NaOH.

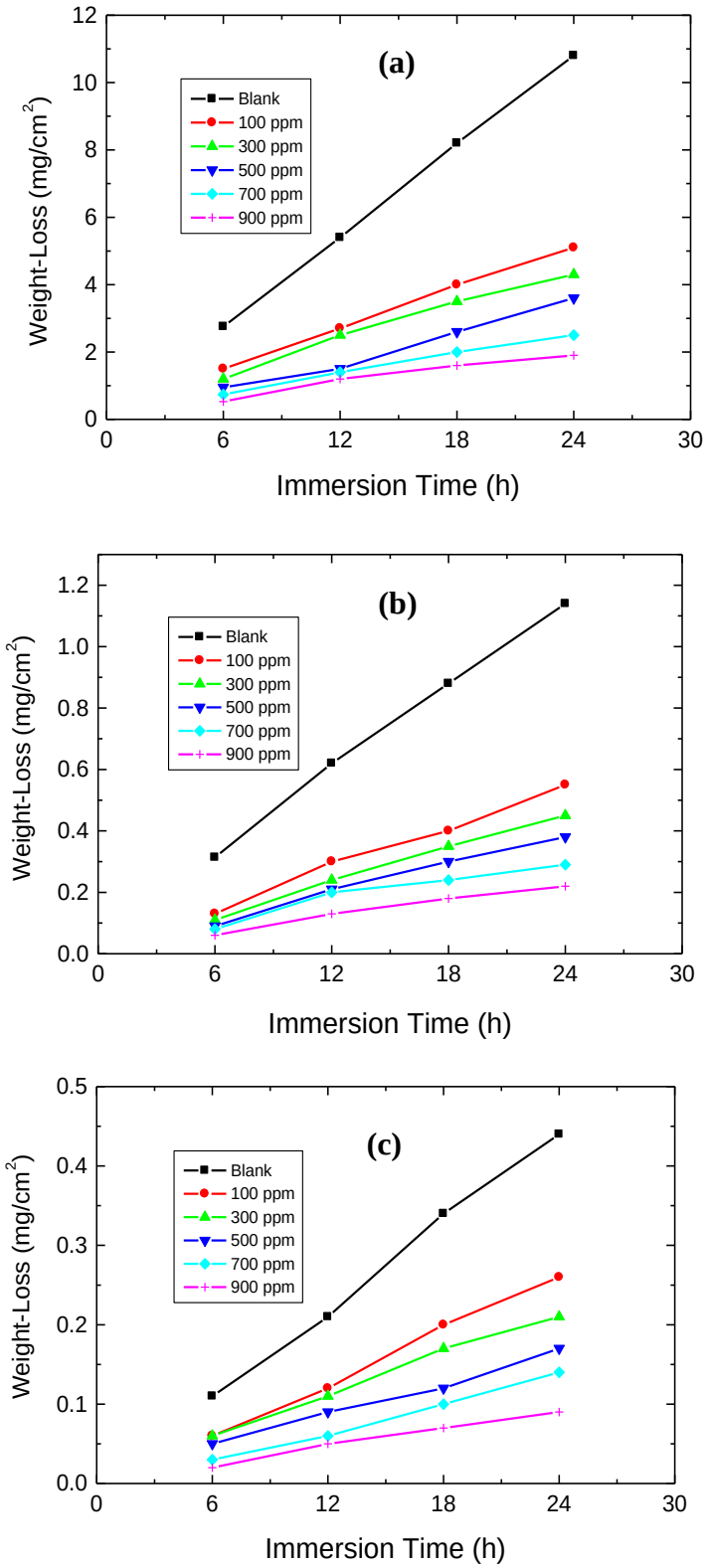

Figure 3. Weight-loss against immersion time for Sabic iron in 0.5 M of the corrosive media: (a) HCl, (b) NaCl and (c) NaOH in the absence and presence of arginine surfactant inhibitor at 25 ^{o}C.

3.1.3. Effect of Temperature

The effect of temperature (15 – 45 ^{o}C) on the CR of Sabic iron in 0.5 M of the corrosive media (HCl, NaCl and NaOH) and on % IE of the synthesized arginine surfactant inhibitor was investigated using WL measurements. Similar curves illustrated in Figure 3 were obtained but not shown here. As the temperature increases, the values of CR and % IE of the additives decrease as listed in Table 3. Decreasing % IE of the synthesized inhibitor in the studied media with rising temperature suggests physical adsorption of the inhibitor on the iron surface [25,26].

Table 3. Corrosion rates (CR) of Sabic iron, θ and % IE of arginine surfactant inhibitor in 0.5 M of the corrosive media (HCl, NaCl and NaOH) at different temperatures.

0.5 M of:	Inhibitor Concn. (ppm)	Temperature (^{o}C)											
		15			25			35			45		
		CR	% IE	θ	CR	% IE	θ	CR	% IE	θ	CR	% IE	θ
HCl	**0**	**178.0**	--	--	**202.0**	--	--	**223.0**	--	--	**244.0**	--	--
	100	72.8	59	0.59	91.1	55	0.55	109.3	51	0.51	136.6	44	0.44
	300	57.1	68	0.68	75.3	63	0.63	91.4	59	0.59	114.7	53	0.53
	500	39.2	78	0.78	58.8	71	0.71	75.8	66	0.66	95.2	61	0.61
	700	26.7	85	0.85	37.9	81	0.81	55.8	75	0.75	68.3	72	0.72
	900	19.6	89	0.89	28.3	86	0.86	46.8	79	0.79	61.0	75	0.75
NaCl	**0**	**19.7**	--	--	**23.1**	--	--	**26.3**	--	--	**30.1**	--	--
	100	7.7	61	0.61	10.7	54	0.54	13.4	49	0.49	17.1	43	0.43
	300	6.3	68	0.68	8.6	63	0.63	11.3	57	0.57	14.4	52	0.52
	500	3.9	80	0.80	5.8	75	0.75	8.2	69	0.69	10.2	66	0.66
	700	2.8	86	0.86	4.7	80	0.80	6.3	76	0.76	9.0	70	0.70
	900	2.6	87	0.87	4.0	83	0.83	5.5	79	0.79	8.4	72	0.72
NaOH	**0**	**7.2**	--	--	**8.2**	--	--	**9.0**	--	--	**9.9**	--	--
	100	4.0	45	0.45	4.9	40	0.40	5.7	37	0.37	6.8	31	0.31
	300	2.7	62	0.62	3.6	56	0.56	4.3	52	0.52	5.2	47	0.47
	500	1.7	77	0.77	2.2	73	0.73	2.8	69	0.69	3.6	64	0.64
	700	1.2	83	0.83	1.8	78	0.78	2.5	72	0.72	3.1	69	0.69
	900	1.1	85	0.85	1.6	80	0.80	2.3	74	0.74	3.0	70	0.70

3.1.4. Adsorption Isotherm

The values of fractional surface coverage (C_{inh}/θ) were plotted versus inhibitor concentrations (C_{inh}) at different temperatures and are illustrated in Figure 4. Straight lines with approximately unit slopes were obtained suggesting that the mode of adsorption of the inhibitor molecules on Sabic iron surface in the corrosive media agrees with the Langmuir adsorption isotherm [27] which is given by:

$$\frac{C_{inh}}{\theta} = \frac{1}{K_{ads}} + C_{inh} \qquad (5)$$

where K_{ads} is the adsorptive equilibrium constant (Table 4).

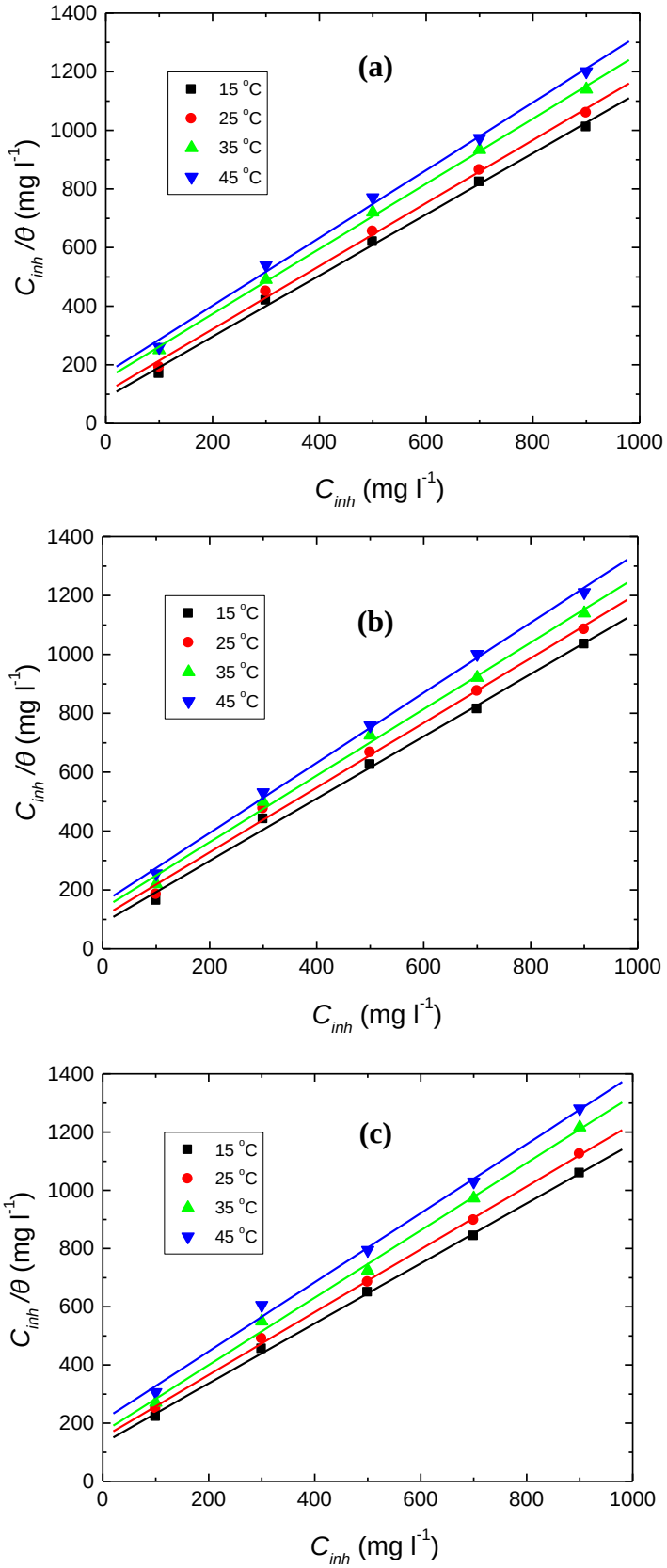

Figure 4. Langmuir adsorption isotherms for arginine surfactant inhibitor adsorbed on Sabic iron surface in 0.5 M of the corrosive media: (a) HCl, (b) NaCl and (c) NaOH, at different temperatures.

3.1.5. Thermodynamic Parameters

Standard free energy (ΔG^{o}_{ads}) is related to K_{ads} according to the equation [28],

$$\Delta G^{o}_{ads} = -RT \ln(55.5\, K_{ads}) \quad (6)$$

The values of ΔG^{o}_{ads} for the studied arginine surfactant inhibitor in the corrosive media (HCl, NaCl and NaOH) were calculated (Table 3). The large negative values of ΔG^{o}_{ads} indicate that the adsorption of arginine inhibitor on Sabic iron surface is spontaneous and stable [29]. The obtained ΔG^{o}_{ads} values indicated that the adsorption mechanism of the synthesized arginine surfactant on Sabic iron in 0.5 M of the corrosive media is a mixed from physical and chemical adsorption [30].

Standard heat of adsorption (ΔH^{o}_{ads}) was calculated using Van't Hoff equation [31]:

$$\ln K_{ads} = \frac{-\Delta H^{o}_{ads}}{RT} + \text{Constant} \quad (7)$$

Plots of ln K_{ads} vs. 1/T yielded good straight lines (Figure 5) and the values of ΔH^{o}_{ads} were evaluated (Table 4). The obtained negative values of ΔH^{o}_{ads} reveal that inhibitor adsorption is an exothermic process with a physical nature [32].

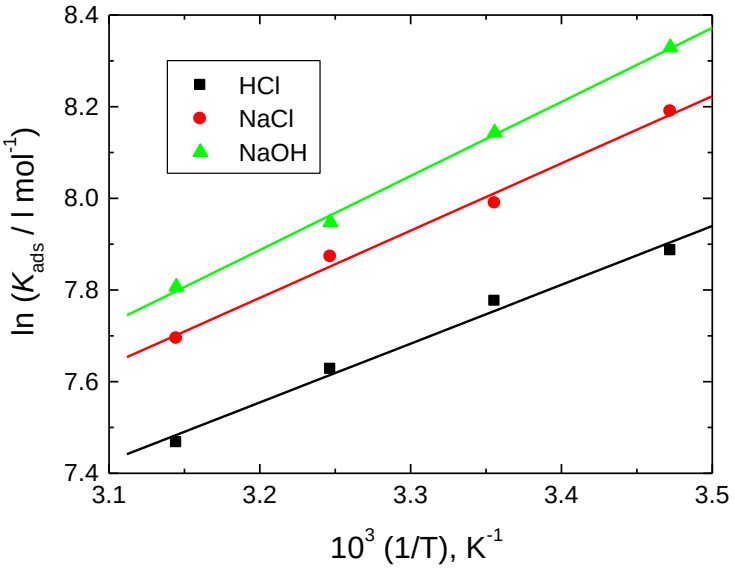

Figure 5. Van't Hoff plots for the arginine surfactant inhibitor adsorbed on Sabic iron surface in 0.5 M of the corrosive media (HCl, NaCl and NaOH).

Standard entropy of adsorption (ΔS^{o}_{ads}) was computed from the equation:

$$\Delta G^{o}_{ads} = \Delta H^{o}_{ads} - T\Delta S^{o}_{ads} \quad (8)$$

The obtained positive values of ΔS^{o}_{ads} (Table 4) showed that the disorder of the inhibitor molecules during their adsorption is increased [33].

Table 4. Thermodynamic parameters and K_{ads} for the corrosion of Sabic iron in 0.5 M of the corrosive media (HCl, NaCl and NaOH), in presence of arginine surfactant inhibitor at different temperatures.

0.5 M of:	Temp. (°C)	10^{-3} K_{ads} l mol^{-1}	ΔG^o_{ads} kJ mol^{-1}	ΔH^o_{ads} kJ mol^{-1}	ΔS^o_{ads} J mol^{-1} K^{-1}
HCl	**15**	2.66	-29.76	-10.66	64.07
	25	2.38	-29.48		63.15
	35	2.05	-29.11		61.91
	45	1.75	-28.71		60.57
NaCl	**15**	3.60	-30.56	-12.21	61.58
	25	2.95	-30.01		59.73
	35	2.63	-29.72		58.76
	45	2.20	-29.28		57.28
NaOH	**15**	4.14	-30.86	-13.43	58.49
	25	3.44	-30.39		56.91
	35	2.83	-29.91		55.30
	45	2.46	-29.56		54.13

3.1.6. Kinetic Parameters

Activation energy (E_a^*) was obtained from Arrhenius equation [34]:

$$\ln CR = \ln A - \frac{E_a^*}{RT} \quad (9)$$

Figure 6 represents the Arrhenius plots for Sabic iron in 0.5 M of the corrosive media (HCl, NaCl and NaOH) in the absence and presence of the synthesized arginine surfactant. The calculated values of E_a^* (Table 5) in the presence of the inhibitor were higher than that in the blank solutions indicating adsorption of the inhibitor molecules on the iron surface and formation of a barrier between the iron surface and the corrosive media. Furthermore, the range of E_a^* values (13.30 – 29.43 kJ mol^{-1}) are lower than 80 kJ mol^{-1} confirming the physical adsorption of the inhibitor [35].

Enthalpy of activation (ΔH^*) and entropy of activation (ΔS^*) for metal corrosion are calculated the equation [36]:

$$\ln\left(\frac{CR}{T}\right) = \left(\ln\frac{R}{Nh} + \frac{\Delta S^*}{R}\right) - \frac{\Delta H^*}{R}\frac{1}{T} \quad (10)$$

where, N is Avogadro's number and h is Planck's constant.

Plots of ln(CR/T) versus 1/T are presented in Figure 7. Values of ΔH^* and ΔS^* are listed in Table 5. The obtained positive values of ΔH^* reflect the endothermic nature of the corrosion process. Also, high values and negative sign of ΔS^* suggesting association of the inhibitor molecules [37].

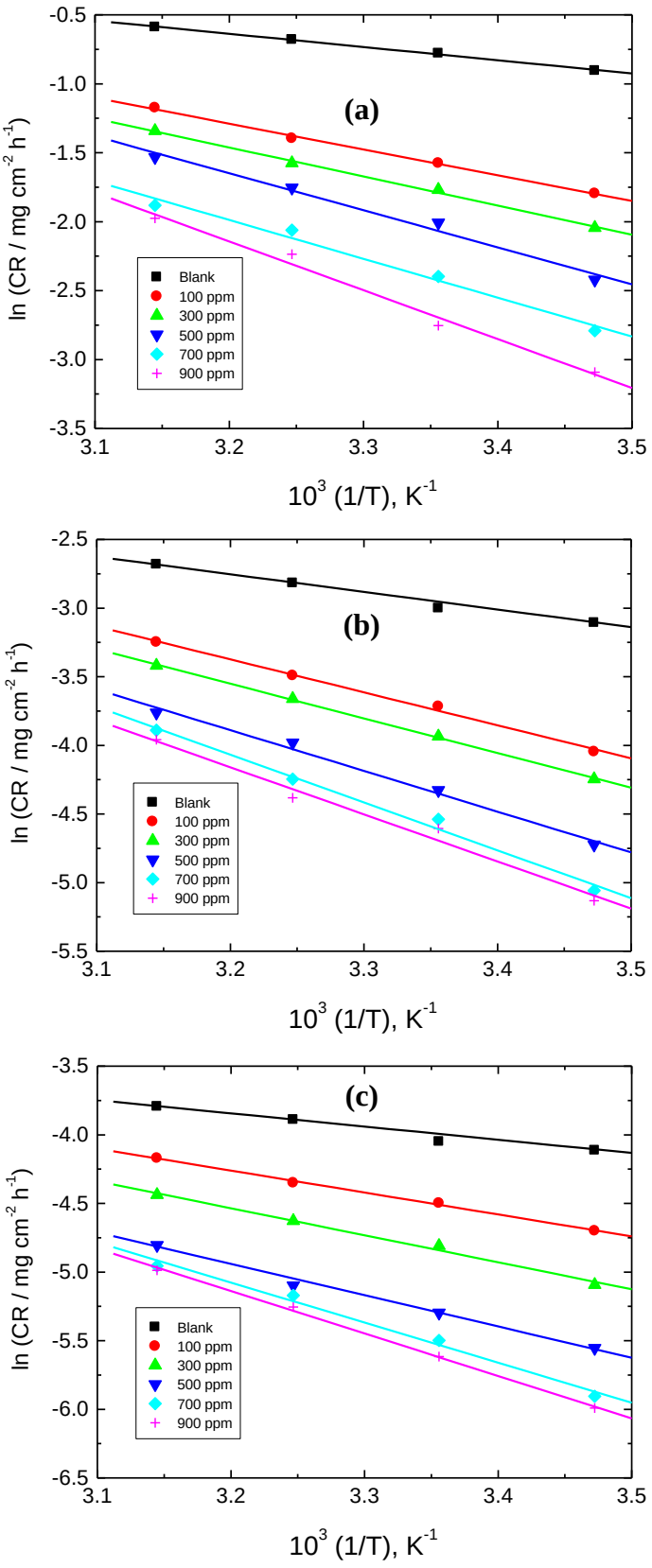

Figure 6. Arrhenius plots for the corrosion of Sabic iron in 0.5 M of the corrosive media: (a) HCl, (b) NaCl and (c) NaOH, in the absence and presence of arginine surfactant inhibitor.

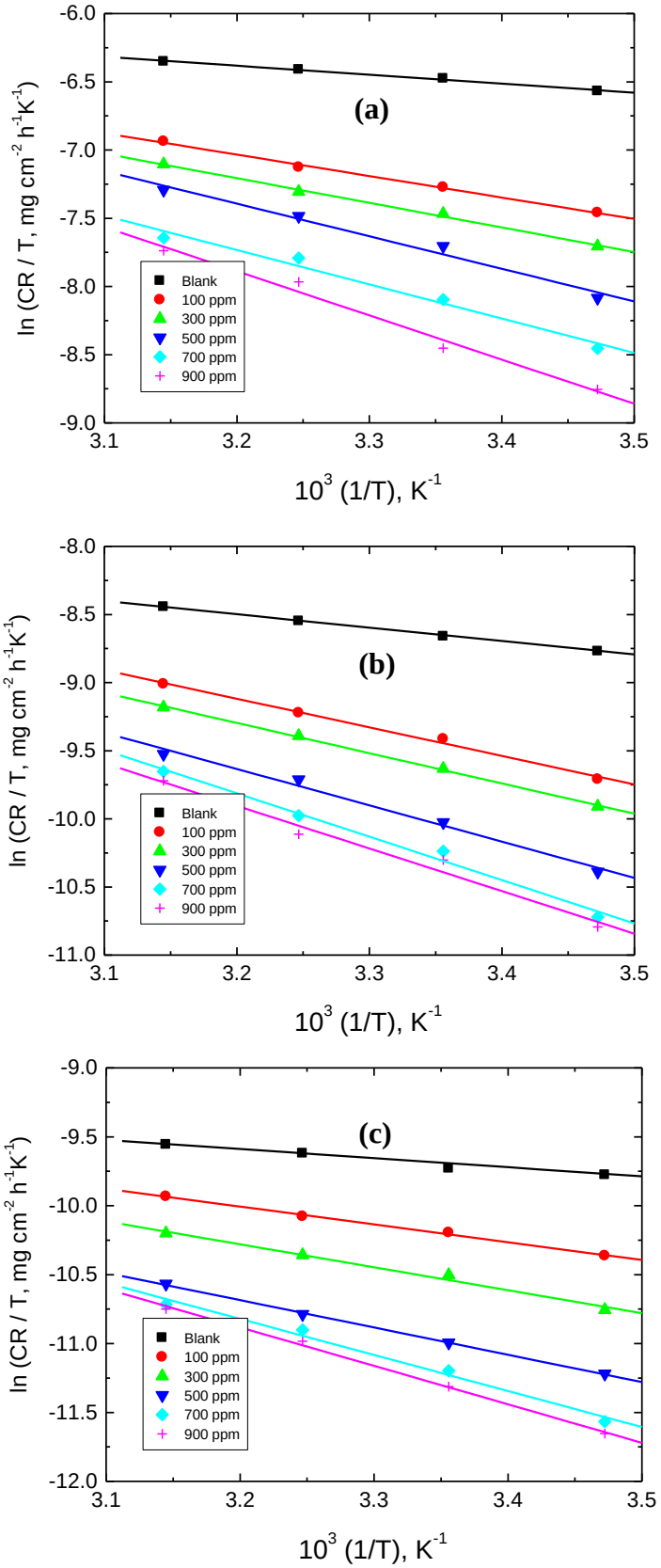

Figure 7. Transition state plots for the corrosion of Sabic iron in 0.5 M of the corrosive media: (a) HCl, (b) NaCl and (c) NaOH, in the absence and presence of arginine surfactant inhibitor.

Table 5. Activation parameters for the corrosion of Sabic iron in 0.5 M of the corrosive media (HCl, NaCl and NaOH), in the absence and presence of arginine surfactant inhibitor.

0.5 M of:	Inhibitors Concn. (mg l^{-1})	E_a^* kJ mol^{-1}	ΔH^* kJ mol^{-1}	ΔS^* J mol^{-1} K^{-1}
--	**0**	**7.98**	**5.40**	**-161.96**
HCl	**100**	15.55	13.05	-180.91
	300	17.46	14.97	-185.65
	500	22.36	19.79	-195.54
	700	23.45	20.78	-194.96
	900	29.43	26.94	-177.00
--	**0**	**10.64**	**8.15**	**-153.06**
NaCl	**100**	20.62	17.38	-177.59
	300	20.95	18.46	-179.33
	500	24.69	22.12	-187.73
	700	28.94	26.44	-194.38
	900	28.60	26.00	-196.71
--	**0**	**8.01**	**5.65**	**-135.43**
NaOH	**100**	13.30	10.73	-148.82
	300	16.38	13.80	-156.39
	500	18.96	16.46	-161.04
	700	24.28	21.70	-177.17
	900	25.69	23.28	-181.41

3.3. Potentiodynamic Polarization (PP) Measurements

3.3.1. Effect of Corrosive Media Concentrations

Figure 8 illustrates Tafel plots recorded for Sabic iron corrosion in HCl, NaCl and NaOH at different concentrations in the range of 0.1 - 1.0 M at 25 ^oC. Values of corrosion potential (E_{corr}), corrosion current density (i_{corr}), cathodic and anodic Tafel slopes (β_c, β_a) were obtained from such plots and are inserted in Table 6. The obtained value of i_{corr} of the investigated Sabic iron was found to increase with increasing the concentration of the corrosive media.

3.3.2. Effect of Inhibitor Concentration

The PP curves for Sabic iron in 0.5 M of the corrosive media (HCl, NaCl and NaOH), in the absence and presence of arginine surfactant inhibitor are illustrated in Figure 9 and the associated corrosion parameters were evaluated and are listed in Table 7. The results showed the inhibitor exhibited anodic and cathodic inhibition effects with anodic predominance [38]. The obtained values of % IE were increased with inhibitor concentration and the extent of inhibition efficiency of the inhibitor, at the same concentration, followed the order: HCl > NaCl > NaOH.

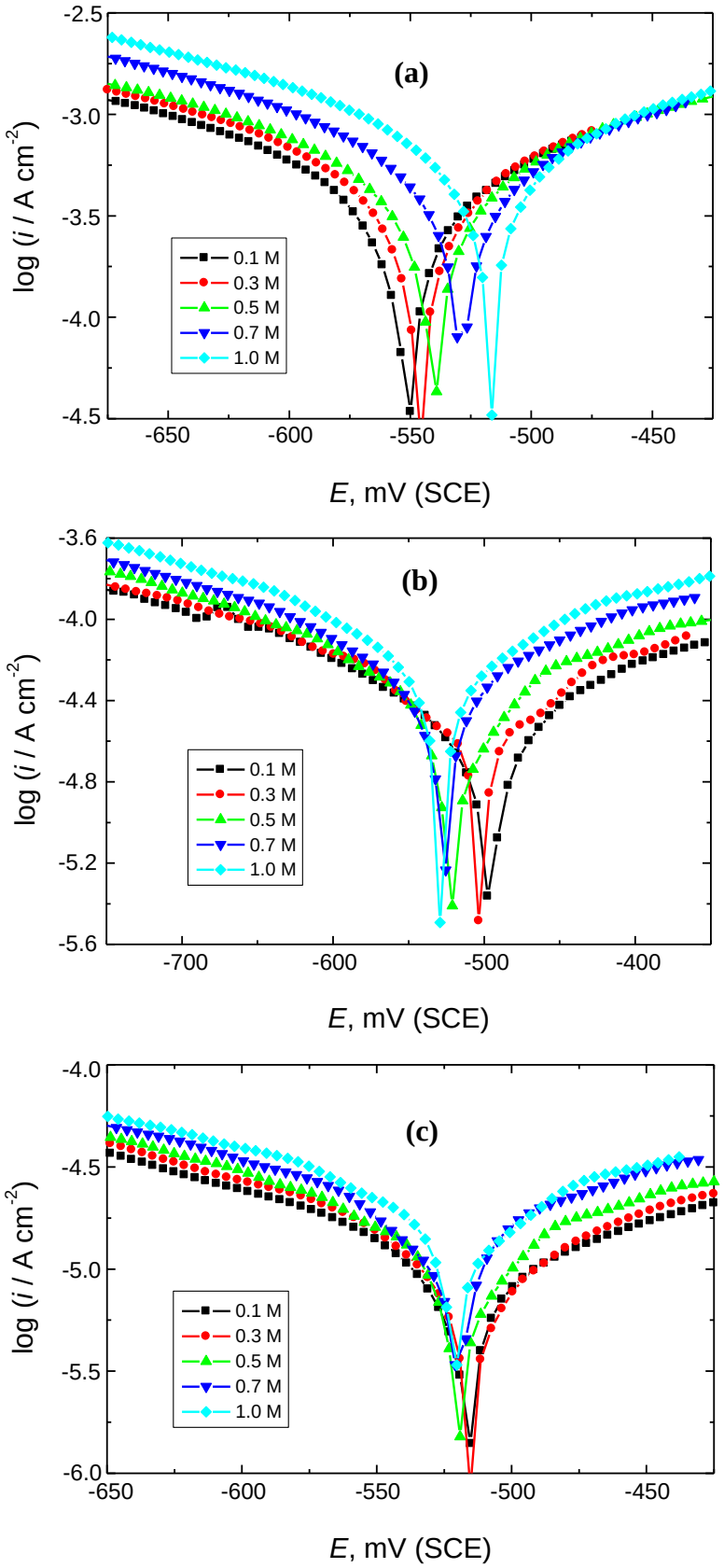

Figure 8. PP curves for the corrosion of Sabic iron in the corrosive media: (a) HCl, (b) NaCl and (c) NaOH at 25 ºC.

Table 6. PP data for Sabic iron in the corrosive media (HCl, NaCl and NaOH) at 25 °C.

Corrosive medium	Concn. (mol dm^{-3})	$-E_{corr}$ (mV(SCE))	β_a (mV/decade)	$-\beta_c$ (mV/decade)	i_{corr} (μA/cm^2)	*CR* (mpy)
HCl	**0.1**	551	228	224	368	167
	0.3	546	219	221	417	186
	0.5	537	211	220	448	202
	0.7	528	190	222	469	206
	1.0	515	166	226	507	223
NaCl	**0.1**	494	318	360	30.2	14.5
	0.3	503	239	372	34.0	18.3
	0.5	527	349	366	40.7	23.1
	0.7	531	342	352	47.3	25.2
	1.0	529	357	363	53.5	29.7
NaOH	**0.1**	515	202	264	11.2	6.3
	0.3	516	193	272	12.7	7.1
	0.5	514	268	259	14.2	8.2
	0.7	517	281	263	16.8	9.2
	1.0	521	266	261	19.3	9.5

Table 7. Polarization data for the corrosion of Sabic iron in 0.5 M of the corrosive media (HCl, NaCl and NaOH), in the absence and presence of the arginine surfactant inhibitor at 25 °C.

0.5 M of	Inhibitor Concn. (ppm)	$-E_{corr}$ (mV(SCE))	β_a (mV/decade)	$-\beta_c$ (mV/decade)	i_{corr} (μA/cm^2)	% IE	θ
HCl	**0**	**537**	**211**	**220**	**448**	--	--
	100	526	118	143	231	48	0.48
	300	523	141	217	173	61	0.61
	500	504	172	215	129	71	0.71
	700	447	181	211	66	85	0.85
	900	436	189	209	33	93	0.93
NaCl	**0**	**527**	**349**	**366**	**40.7**	--	--
	100	529	203	207	21.1	48	0.48
	300	521	297	239	16.2	60	0.60
	500	492	287	176	11.2	72	0.72
	700	507	278	211	7.1	83	0.83
	900	508	304	225	4.2	90	0.90
NaOH	**0**	**514**	**268**	**259**	**14.2**	--	--
	100	511	278	252	8.9	37	0.37
	300	508	211	177	5.8	59	0.59
	500	510	197	238	3.6	75	0.75
	700	510	184	233	2.7	81	0.81
	900	504	199	247	2.2	85	0.85

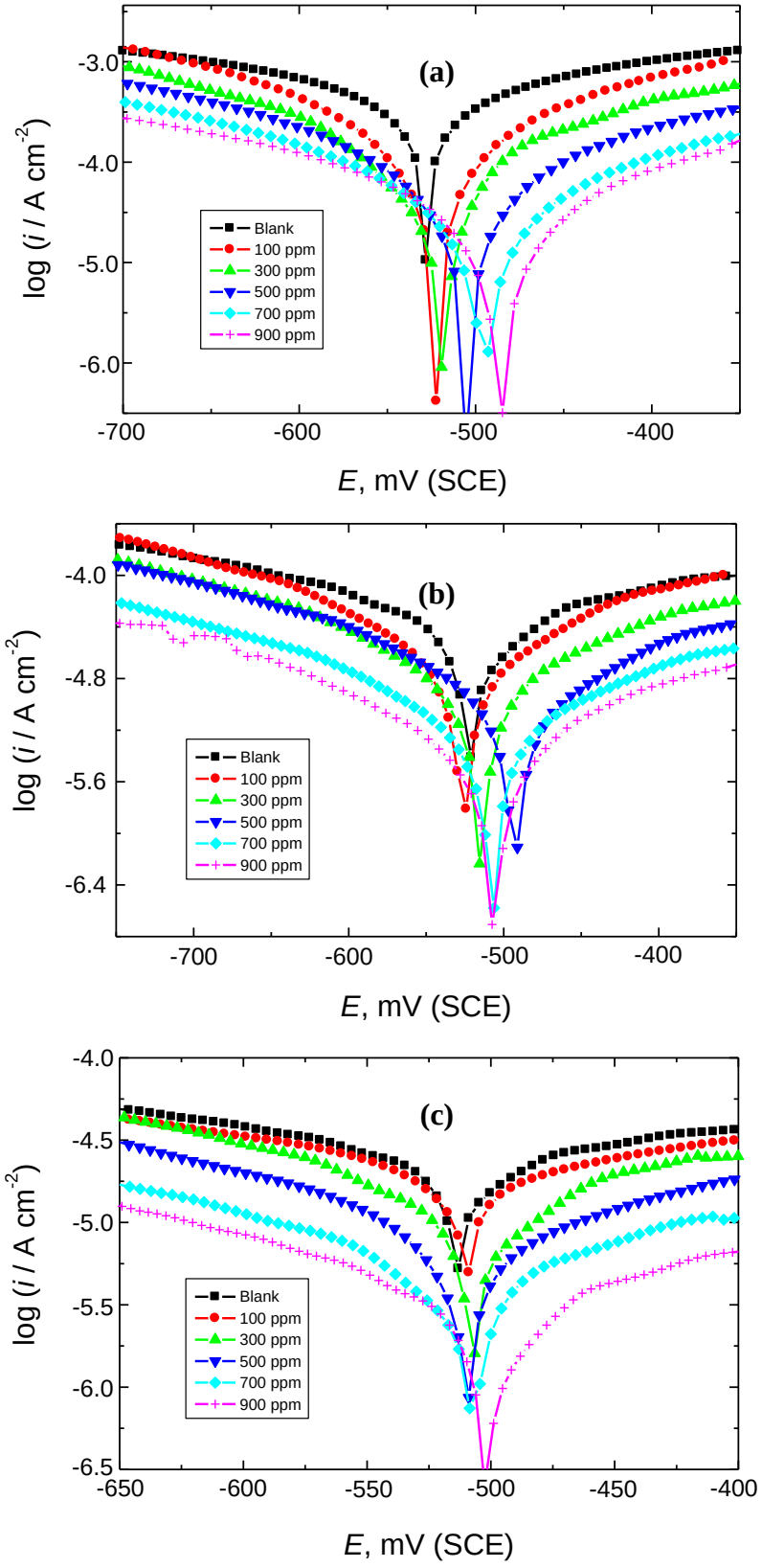

Figure 9. PP curves for Sabic iron corrosion in 0.5 M of the corrosive media: (a) HCl, (b) NaCl and (c) NaOH, in the absence and presence of arginine surfactant inhibitor at 25 ^{o}C.

3.4. Electrochemical Impedance Spectroscopy (EIS) Measurements

Corrosion behavior of Sabic iron in 0.5 M of the corrosive media (HCl, NaCl and NaOH) has been also investigated in the absence and presence of the synthesized inhibitor at 25 ^{o}C by EIS. Nyquist plots obtained for Sabic iron at different concentrations of the inhibitor are shown in Figure 10. The values of R_{ct}, IE % and θ are listed in Table 8. It has been observed that the size of the capacitive semicircle of Sabic iron in the corrosive media increased significantly after the addition of the inhibitor indicating a decrease in the rate of corrosion, and this behavior increased as the inhibitor concentration increased [39].

Table 8. Values of R_{ct} and % IE of the arginine surfactant inhibitor for the corrosion of Sabic iron in 0.5 M of the corrosive media (HCl, NaCl and NaOH), at 25 ^{o}C.

Inhibitor Concn. (ppm)	HCl		NaCl		NaOH	
	R_{ct}	% IE	R_{ct}	% IE	R_{ct}	% IE
0	**66**	**--**	**285**	**--**	**440**	**--**
100	137	52	560	49	745	41
300	173	62	731	61	977	55
500	254	74	1022	72	1570	72
700	471	86	1585	82	2095	79
900	662	90	1908	85	2590	83

3.5. Surface Investigations

Scanning electron microscopy (SEM) images of Sabic iron specimens in 0.5 M of the corrosive media (HCl, NaCl and NaOH) in the absence and presence of a 900 ppm of the examined inhibitor are shown in Fig. 11. Figure 11a shows pure Sabic iron surface before immersion in the corrosive media. Figure 11(b1–b3) and (c1–c3) shows Sabic iron surface after immersion in 0.5 M of the corrosive media for 12 h, in the absence and presence of 900 ppm of the inhibitor, respectively. From Figure 11b, it can be observed that Sabic iron surface was corroded in the examined corrosive media and the extent of the surface corrosion was found in the order: HCl > NaCl > NaOH, in consistent with the results obtained. Figure 11c manifests SEM images of Sabic iron surface after addition of a 900 ppm of the synthesized inhibitor to the corrosive media which shows that the surface of Sabic iron was suffered a remarkable change and was widely covered with the inhibitor molecules. This is an indication of strong adsorption of the inhibitor molecules on Sabic iron surface leading to an excellent corrosion inhibition [40].

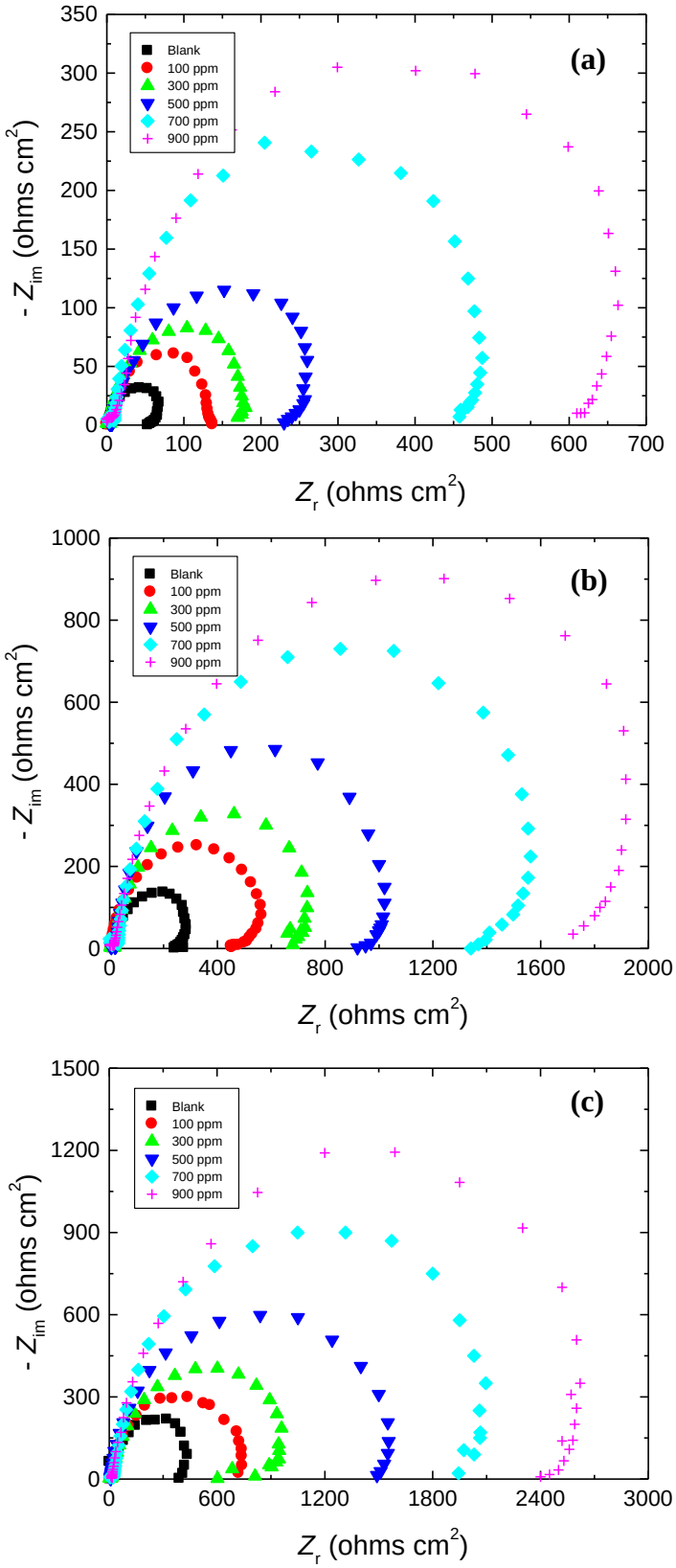

Figure 10. Nyquist plots for the corrosion of Sabic iron in 0.5 M of the corrosive media (HCl, NaCl and NaOH), in the absence and presence of the arginine surfactant inhibitor at 25 ^{o}C.

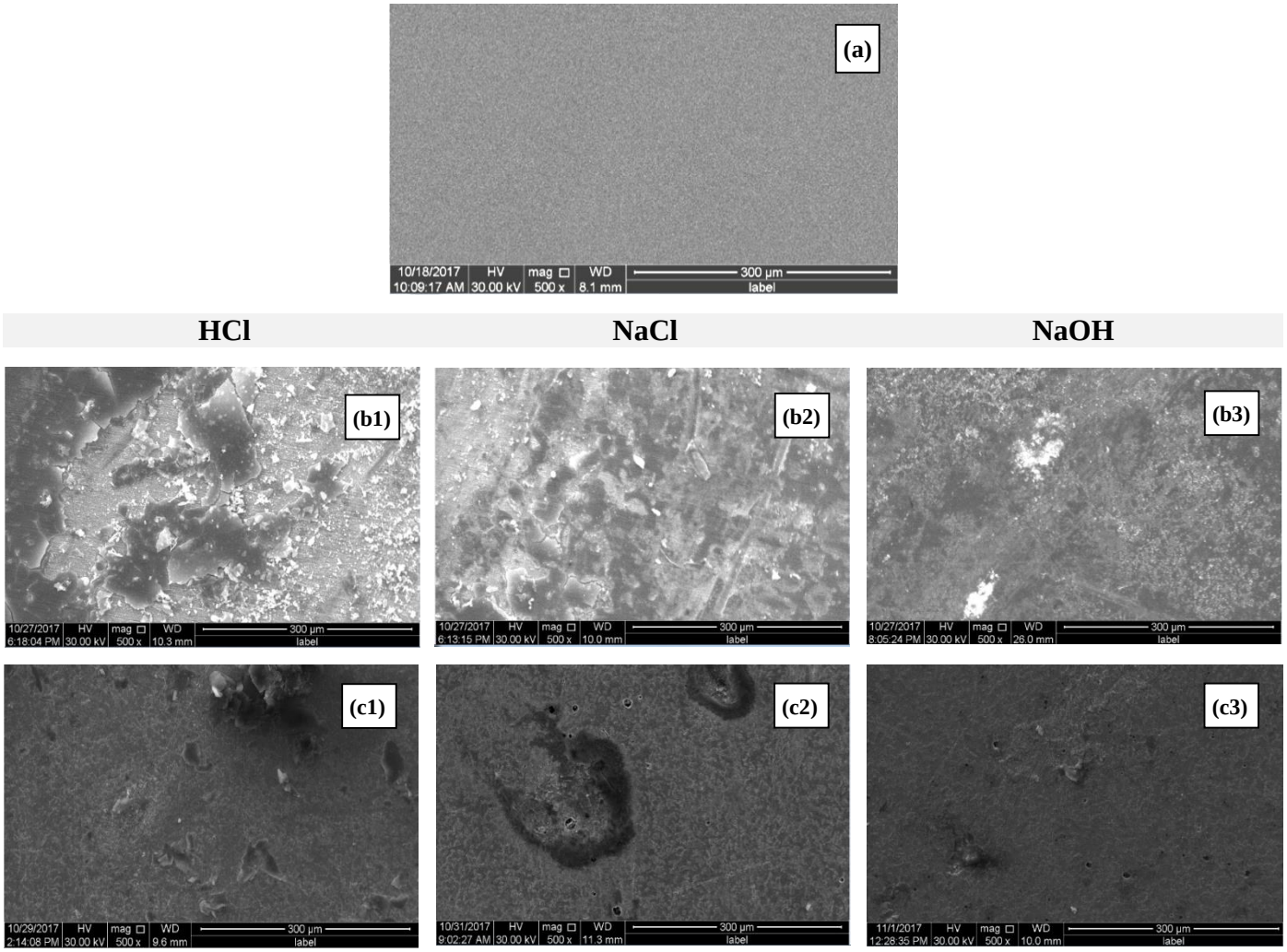

Figure 11. SEM micrographs of Sabic iron surface: (a) before immersion in the corrosive media, (b) after 12 h immersion in 0.5 M of the corrosive media: (b1) HCl, (b2) NaCl and (b3) NaOH, and (c1, c2 and c3) after 12 h immersion in the corrosive media containing 900 ppm of arginine surfactant inhibitor.

4. CONCLUSIONS

1) The new synthesized sodium N-dodecyl arginine surfactant was used as an excellent inhibitor for the corrosion of Sabic iron in the corrosive media; HCl, NaCl and NaOH.

2) The corrosion rate of Sabic iron increased in the order: HCl >> NaCl > NaOH.

3) Adsorption of the synthesized inhibitor on Sabic iron follows the Langmuir adsorption isotherms.

4) Adsorption process of the inhibitor is spontaneous and endothermic, and the adsorption type is physical.

ACKNOWLEDGMENTS
The authors would like to thank the Deanship of Scientific Research at Umm Al-Qura University for the financial support (Grant code 15-SCI-3-1-0014).

References

1. R.F. Godec and M.G. Pavlovic, *Corros. Sci.*, 58 (2012) 192.
2. M. Abdallah, O.A. Hazazi, A. Fawzy, S. El-Shafei and A. S. Fouda, *Prot. Met. Phys. Chem. Surf.*, 50 (2014) 659.
3. M.I. Awad, A.F. Saad, M.R. Shaaban, B.A. AL-Jahdaly and O.A. Hazazi, *Int. J. Electrochem. Sci.*, 12 (2017) 1657.
4. O.A. Hazazi, A. Fawzy, M.R. Shaaban and M.I. Awad, *Int. J. Electrochem. Sci.*, 9 (2014) 1378.
5. M. Abdallah, A.S. Fouda, I. Zaafarany, A. Fawzy and Y. Abdallah, *J. Am. Sci.*, 9 (2013) 209.
6. M. Abdallah, I. Zaafarany, A. Fawzy, M.A. Radwan and E. Abdfattah, *J. Am. Sci.*, 9 (2013) 580.
7. O.A. Hazazi, A. Fawzy and M.I. Awad, *Chem. Sci. Rev. Lett.*, 4 (2015) 67.
8. M. Abdallah, M.M. Salem, B.A.AL-Jahdaly, M.I. Awad, E. Helal and A.S. Fouda, *Int. J. Electrochem Sci.*, 12 (2017) 4543.
9. M. Abdallah, M.M. Salem, A. Fawzy and E.M. Mabrouk, *J. Mater. Env. Sci.*, 8 (2017) 1320.
10. R. Fuchs-Godec, *Electrochim. Acta*, 54 (2009) 2171.
11. N.A. Negm and F.M. Zaki, *Coll. Surf. A*, 322 (2008) 97.
12. X. Li, S. Deng, G. Mu, H. Fu and F. Yang, *Corros. Sci.*, 50 (2008) 420.
13. L. Rodrigues, I.M. Banat, J. Teixeira and R. Oliveira, *J. Antimicrob. Chemother.*, 57 (2006) 609.
14. P. Singh and S.S. Cameotra, *Trends Biotechnol.*, 22 (2004) 142.
15. P. Clapés and M.R. Infante, *Biocatal. Biotransform.*, 20 (2002) 215.
16. L. Pérez, J.L. Torres, A. Manresa, C. Solans and M.R. Infante, *Langmuir*, 12 (1996) 5296.
17. L. Pérez, A. Pinazo, P. Vinardell, P. Clapés, M. Angelet and M.R. Infante, *New J. Chem.*, 26 (2002) 1221.
18. Y. Le, in "Synthesis and physicochemical study of novel amino acid based surfactants" Master Thesis, Göteborg, Sweden, p. 2, 2011.
19. A. Fawzy, I.A. Zaafarany, H.M. Ali and M. Abdallah, *Int. J. Electrochem Sci.*, 13 (2018) 4575.
20. A. Fawzy, M. Abdallah, I. A. Zaafarany, S.A. Ahmed and I. I. Althagafi, *J. Mol. Liq.*, 265 (2018) 276.
21. H. Tapiero, G. Mathé, P. Couvreur and K.D. Tew, *Biomed. Pharmacother.*, 56 (2002) 439.
22. L.B. Tang, G.N. Mu and G.H. Liu, Corros. Sci., 45 (2003) 2251.
23. P. Manjula, S. Manonmani, P. Jayaram and S. Rajendran, *Anti-Corros. Methods Mater.*, 48 (2001) 319.
24. H. Ma, S. Chen, L. Niu, S. Zhao, S. Li and D. Li, *J. Appl. Electrochem*., 32 (2002) 65.
25. M. Erbil, *Chim. Acta Turc.*, 1 (1988) 59.
26. F. Touhami, A. Aouniti, Y. Abed, B. Hammouti, S. Kertit, A. Ramdani and K. Elkacemi, *Corros. Sci.*, 42 (2000) 929.
27. M. Christov and A. Popova, *Corros. Sci.*, 46 (2004) 1613.
28. S.K. Shukla and M.A. Quraishi, *Corros. Sci.*, 51 (2009) 1007.
29. M. Abdallah, M. Sobhi and H.M. Altass, *J. Mol. Liq.*, 223 (2016) 1143.
30. P.C. Okafor and Y. Zheng, *Corros. Sci.*, 51 (2009) 850.
31. T.P. Zhao and G.N. Mu, *Corros. Sci.*, 41 (1999) 1937.
32. F. Bentiss, M. Traisnel and M. Lagrenee, *Corros Sci.*, 42 (2000) 127.
33. W. Durnie, R.D. Marco, A. Jefferson and B. Kinsella, *J. Electrochem. Soc.*, 146 (1999) 1751.
34. M. Elachouri, M.S. Hajji, M. Salem, S. Kertit, J. Aride, R. Coudert and E. Essassi, *Corrosion*, 52 (1996) 103.

35. B. Xu, Y. Liu, X. Yin, W. Yang and Y. Chen, *Corros. Sci.*, 74 (2013) 206.
36. J.O.M. Bockris and A.K.N. Reddy, Modern Electrochemistry, vol. 2, Plenum Press, New York, 1977.
37. J. Marsh, Advanced Organic Chemistry, 3rd ed., Wiley, Eastern New Delhi, 1988.
38. G.N. Mu, X.H. Li and Q. Qu, J. Zhou, *Corros. Sci.*, 48 (2006) 445.
39. C. Hsu and F. Mansfeld, *Corrosion*, 57 (2001) 747.
40. R.A. Prabhu, T.V. Venkatesha, A.V. Shanbhag, G.M. Kulkarni and R.G. Kalkhambkar, *Corros. Sci.*, 50 (2008) 3356.